**Applied and Environmental Microbiology**

# A class IV adenylate cyclase CyaB is required for capsule polysaccharide production and biofilm formation in *Vibrio parahaemolyticus*

**Regmi, A., J.G. Tague, and E.F. Boyd***

Department of Biological Sciences, University of Delaware, Newark, DE 19716

Corresponding author*

E. Fidelma Boyd

Department of Biological Sciences

341 Wolf Hall, University of Delaware

Newark, DE 19716

Phone: (302) 831-1088. Fax: (302) 831-2281 Email: fboyd@udel.edu

**ABSTRACT**

CRP (cyclic AMP receptor protein), encoded by *crp*, is a global transcription factor that is activated by cyclic AMP (cAMP), a second messenger synthesized from ATP by adenylate cyclase, *cyaA* in *Escherichia coli*. In this species, growth on the preferred carbon source glucose, results in low levels of cAMP, and inactive CRP. When glucose is absent, cAMP levels are high which activates CRP to regulate 100s of genes. To investigate the role of CRP in *Vibrio parahaemolyticus*, we constructed non-polar deletions of the *crp* and *cyaA* homologs. The Δ*crp* mutant did not grow in minimal media supplemented with non-glucose carbon sources, however the Δ*cyaA* mutant grew similar to wild type suggesting the presence of an additional adenylate cyclase. Bioinformatics analysis identified a homolog of a class IV adenylate cyclase, CyaB present in *V. parahaemolyticus*. Both *V. parahaemolyticus cyaA* and *cyaB* functionally complemented an *E. coli* Δ*cyaA* mutant indicating adenylate cyclase activity. Growth pattern analysis showed that *cyaA* is controlled by CRP, but *cyaB* is not. cAMP-CRP was required for motility with the Δ*crp* and Δ*cyaB*/Δ*cyaA* mutants having a defect in swimming and swarming motility. The Δ*cyaA* mutant produces capsule polysaccharide (CPS) and biofilm similar to wild type. However, the Δ*cyaB* mutant was defective in CPS production and biofilm formation, similar to the Δ*crp* and Δ*cyaB*/Δ*cyaA* mutants, indicating that CyaB, but not CyaA, is required for these phenotypes. Phylogenetic analysis of *cyaB* showed broad distribution within the *Vibrionaceae* family and was acquired by horizontal gene transfer in several species.

42 **IMPORTANCE**

43 The physiological role of class IV adenylate cyclases remains unknown and previously
44 only a class I adenylate cyclase was identified within *Vibrio* species. Here we identify
45 and characterize a class IV AC in *V. parahaemolyticus*. Our analysis shows that CyaB is
46 essential for optimal growth and is required for capsule polysaccharide production and
47 biofilm formation. The *cyaB* gene is widespread among *Vibrionaceae* species and
48 phylogenetic analysis demonstrates that in some species the *cyaB* gene was acquired by
49 horizontal gene transfer.

50

51 **INTRODUCTION**

52 Many bacterial species repress alternative carbon catabolism gene expression when
53 glucose is present, a mechanism known as carbon catabolite repression (CCR) (1). Two
54 major players involved in CCR are adenylate cyclase (AC) encoded by *cyaA*, which
55 produces cyclic AMP (cAMP) from ATP, and the global regulator CRP (**c**AMP **R**eceptor
56 **P**rotein) encoded by *crp*. cAMP is a second messenger that activates CRP, which
57 functions as a homodimer, and in *Escherichia coli* is a global regulator of metabolism (2-
58 4). The CRP regulon includes genes for the transport and catabolism of non-glucose
59 carbon sources. In *E. coli*, the 209 amino acid CRP protein has an N-terminal cAMP
60 binding domain (CBD; residues 1–136) and a C-terminal helix turn helix DNA binding
61 domain (DBD; residues 139–209) (5, 6). When bound by cAMP, CRP undergoes a
62 conformation change that allows the protein to interact with target promoter regions at
63 consensus sequences, a CRP-box consisting of a palindromic 16-bp sequence
64 TGT**G**ANNNNNNT**C**ACA (5, 7). Analysis of 323 CRP-binding sites showed that G at
65 position 4 and C at position 13 of the CRP-box are highly conserved (8). Also, in *E. coli* it
66 was shown that CRP can bind cGMP, but this does not result in transcriptional changes
67 or the conformational change required for DNA binding (9).

68 There are six classes (I-VI) of adenylate cyclases (AC) based on primary amino
69 acid sequence, with different catalytic mechanisms and structures indicating different
70 evolutionary origins (10, 11). *Escherichia coli* and many other *Gamma-Proteobacteria*

71 contain a single adenylate cyclase gene *cyaA*, which encodes a class I AC (AC-I). The 810
72 amino acid CyaA protein has two functionally distinct domains; the N-terminal
73 catalytic cyclase domain and the C-terminal regulatory domain. Studies in *Vibrio* species
74 have shown an expanded physiological role of CyaA in bacteria, specifically in
75 virulence, biofilm formation, motility and type III secretion regulation (12-17). In
76 addition, the regulatory role of CyaA is amplified by its regulation of other global
77 regulators such as the stress response sigma factor RpoS and quorum sensing LuxR
78 homologs. Class II ACs (AC-II) are comprised of bacterial exotoxins such as the
79 calmodulin-activated exotoxin from *Bordetella pertussis*, with an N-terminal cyclase
80 catalytic domain and a C-terminal hemolytic domain (18). The class III ACs are the most
81 diverse and widespread and encompass adenylate cyclases and guanylate cyclases
82 (GCs) from eukaryotic and prokaryotic species (19). A well-characterized AC-III
83 enzyme from bacteria is CyaC from *Pseudomonas aeruginosa* that has receptor binding
84 activity as well as cyclase activity. This species also contains a class I and a class II AC
85 (20). A class IV AC was first described in *Aeromonas hydrophila* and named CyaB, and is
86 a small 181 amino acid protein with unusual alkalinophilic and thermophilic activity (21).
87 An AC-IV was also described in *Yersinia pestis* and its structure determined (22). In
88 *Shewanella oneidensis* MR-1, an AC-IV was identified and shown to have adenylate
89 cyclase activity. This species also contains AC-I encode by *cyaA* and an AC-III encoded
90 by *cyaC* (23). The physiological role of AC-IVs among bacteria is unknown. A

91 structurally diverse AC was identified in *Prevotella ruminicola* D31d and forms the sole
92 representative of AC-V (24). A class VI AC was described in *Rhizobium elti* and was
93 shown to have cyclase activity by complementation of an *E. coli cyaA* mutant (25).
94 Similar to *E. coli*, *V. cholerae*, a human gastrointestinal pathogen, has a single AC,
95 a CyaA homolog that synthesizes cAMP, which binds to CRP to activate transcription
96 (17). cAMP-CRP was shown to play a crucial role in controlling virulence gene
97 expression, biofilm formation and quorum sensing in *V. cholerae* through positive
98 regulation of *hapR (luxR* homolog*)*, the quorum sensing master regulator (12, 17, 26).
99 HapR is a negative regulator of cholera toxin encoded *ctxAB* and the toxin co-regulated
100 pilus encoded by *tcp* as well as biofilm formation in this species. HapR is a repressor of
101 AphA, which is a positive regulator of the *ctxAB* and *tcp* genes, and AphA positively
102 regulates VpsR, a positive regulator of the *vsp* loci required for capsule polysaccharide
103 (CPS) formation and biofilm (12, 27, 28). Thus, HapR and cAMP-CRP are negative
104 regulators of CT and TCP expression and biofilm formation (17, 26). In *V. cholerae*,
105 transcriptomic analysis demonstrated that CRP is a global regulator controlling 176
106 genes (17). A recent study using ChIP-Seq demonstrated 119 CRP binding sites in the
107 genome of *V. cholerae*, most overlapping with previously identified cAMP-CRP binding
108 sites (29).
109 *Vibrio parahaemolyticus* is a halophile present in the marine environment, where it
110 exists free living or associated with marine flora and fauna, forming biofilms (30-32). V.

111 *parahaemolyticus* is also an important human pathogen associated with pandemic
112 infectious disease. Consumption of raw or undercooked shellfish infected with *V.*
113 *parahaemolyticus* causes gastroenteritis in human and is the leading cause of bacterial
114 seafood borne gastroenteritis worldwide (32, 33). In this species, the QS master
115 regulator OpaR (LuxR homolog) positively regulates biofilm by directly, positively
116 regulating *cpsQ* and the *cspA-K* loci required for CPS production, a major component of
117 biofilm (34-40). The role of cAMP-CRP in *V. parahaemolyticus* physiology has not been
118 previously examined.

119 In the present study, the function and activation of CRP in *V. parahaemolyticus*
120 was investigated. We constructed in-frame non-polar deletions of *crp* (VP2793) and *cyaA*
121 (VP2987) homologs in *V. parahaemolyticus* RIMD2201633 and examined their growth
122 patterns in various carbon sources. The Δ*crp* mutant grew on minimal medium M9 3%
123 NaCl (M9) supplemented with glucose (M9G), but was unable to grow on L-arabinose,
124 L- ribose, or D-gluconate as sole carbon sources. The Δ*crp* mutant also showed defects
125 in both swimming and swarming motility. Interestingly, the Δ*cyaA* mutant grew on all
126 carbon sources similar to wild type and showed no motility defects. This suggested the
127 presence of an additional uncharacterized adenylate cyclase gene in *V. parahaemolyticus*.
128 Bioinformatics analysis identified ORF VP1760 that encoded a putative class IV AC,
129 which we named *cyaB*, present in all *V. parahaemolyticus* strains, but absent from most *V.*
130 *cholerae* strains. Both *cyaA* and *cyaB* functionally complemented an *E. coli* Δ*cyaA* mutant.

131 In growth pattern analysis, the Δ*cyaB* and Δ*cyaA* mutants showed significantly different
132 growth curves from each other on all media examined. In addition, the Δ*cyaB* mutant
133 showed significantly different growth patterns depending on the growth media used
134 for overnight cultures used for inoculations. In motility assays, both Δ*cyaA* and Δ*cyaB*
135 mutants behaved similar to wild type, but the double Δ*cyaB*/Δ*cyaA* mutant showed
136 growth and motility defects similar to the Δ*crp* mutant. Next, we examined whether
137 cAMP-CRP played a role in CPS and biofilm formation. The Δ*crp* mutant showed
138 smooth translucent colony morphology demonstrating a lack of CPS, indicating that
139 cAMP-CRP is a positive regulator of CPS. The Δ*cyaA* mutant produced CPS similar to
140 wild type with a rough rugose morphology, however the Δ*cyaB* showed a smooth
141 translucent colony morphology, indicating a lack of CPS. Similarly, in biofilm assays,
142 the Δ*cyaA* mutant produced a biofilm similar to wild type whereas the Δ*crp*, Δ*cyaB*, and
143 Δ*cyaB*/Δ*cyaA* mutants produce significantly less biofilm. Thus, our data show that
144 cAMP-CRP modulates CPS and biofilm and CyaB is essential for this function.
145 Phylogenetic analysis of the *cyaB* gene showed it is phylogenetically widespread among
146 the family *Vibrionaceae* and has been acquired by horizontal gene transfer in many
147 species.

148 **RESULTS**

149 **CRP is an essential regulator in *V. parahaemolyticus*.**

150 cAMP-CRP is a global regulator of nutrient transport in many bacterial species (7-9, 13,
151 15, 17). Homologs of CRP and CyaA are present in *V. parahaemolyticus*, ORF VP2793 and
152 VP2987, respectively (**Fig. S1**). The CRP protein of *V. parahaemolyticus* shared 98% amino
153 acid identity to CRP in *V. cholerae*. The CyaA shared 82% amino acid identity with that
154 of *V. cholerae*. The genome context of both genes was conserved across *V.*
155 *parahaemolyticus*, *V. cholerae* and *E. coli* (**Fig. S1**). To begin to investigate the
156 physiological role of CRP in *V. parahaemolyticus,* we first constructed an in-frame non-
157 polar deletion of *crp* (VP2793) and *cyaA* (VP2987) in *V. parahaemolyticus* RIMD2210633.
158 The Δ*crp* mutant displayed a small colony morphology on LBS plates **(Fig. S2A)**.
159 Growth pattern analysis in LBS broth and M9S D-glucose broth demonstrated that the
160 Δ*crp* strain had a growth defect **(Fig. 1A**-**B**). We examined the effects of deleting *cyaA*,
161 predicting it should behave similar to the Δ*crp* deletion mutant, as seen in *E. coli* and *V.*
162 *cholerae* Δ*cyaA* mutants. Growth of Δ*cyaA* on LBS plates showed identical colony
163 morphology to wild type (**Fig. S2A)** and the growth pattern of Δ*cyaA* in LBS and M9S
164 D-glucose broth showed a similar pattern to wild type (**Fig. 1A**-**B**).
165 Next, we examined growth in alternative carbon sources and found that in M9S
166 supplemented with L-arabinose, L- ribose, or D-gluconate, the Δ*crp* strain was unable to
167 grow (**Fig 2A-C**). These data demonstrate that CRP is required for catabolism of
168 alternative carbon sources similar to many other species. Growth analysis of the Δ*cyaA*
169 mutant in M9S supplemented with L-arabinose, L- ribose, or D-gluconate, showed that

170 it grew similar to wild type (**Fig 2A-C**). These data suggested that *V. parahaemolyticus*
171 contained an additional uncharacterized adenylate cyclase that could synthesize cAMP
172 in the absence of *cyaA*. Alternatively, though less likely, CRP could act independently of
173 cAMP.

174 **Identification of a class IV adenylate cyclase CyaB in *V. parahaemolyticus*.**

175 BLAST analysis using CyaA as a seed to search the RIMD2210633 genome, only hit to
176 itself, indicating no other homolog of the class I adenylate cyclase was present. We then
177 searched the *V. parahaemolyticus* genome for class II, III and class IV adenylate cyclases
178 and identified a homolog of a class IV adenylate cyclase, which we named CyaB. No
179 additional adenylate cyclases were identified in *V. parahaemolyticus*. The CyaB protein
180 shared 45% amino acid identity with CyaB of *Y. pestis* and 56% amino acid identity with
181 CyaB of *A. hydrophila* (**Fig. S3**). In both of these species, the CyaB protein has been
182 structurally characterized and shown to have AC activity generating cAMP, however its
183 physiological role is unknown (21, 22, 41, 42). CyaB lacks transmembrane domains and
184 signal peptide cleavage sites indicating it is a cytosolic protein. To determine whether *V.*
185 *parahaemolyticus* CyaB produces cAMP, we functionally complemented an *E. coli* Δ*cyaA*
186 mutant with either *V. parahaemolyticus cyaA* or *cyaB* and examined growth in D-glucose
187 and D-gluconate. The *E. coli ΔcyaA* did not demonstrate growth defect in D-glucose, but
188 was defective in growth in D-gluconate **(Fig. 3A-B)**. The growth defect of E. *coli ΔcyaA*
189 in D-gluconate was rescued by E. *coli ΔcyaA* strain complemented by either *V.*

190 *parahaemolyticus cyaA* (VP2987) or *cyaB* (VP1760*),* indicating both, CyaA and CyaB, have
191 adenylate cyclase activity (**Fig. 3A-B)**.
192 We reasoned that our lack of Δ*cyaA* mutant phenotypes was due to *cyaB*
193 complementing the Δ*cyaA* mutant. To investigate this further, we constructed a Δ*cyaB*
194 strain and examined growth. The Δ*cyaB* mutant had similar colony morphology to wild
195 type (**Fig. S2A**) and showed identical growth patterns in LBS to wild type **(Fig. 1)**.
196 However, when the Δ*cyaB* mutant was grown overnight in M9S D-glucose and used to
197 inoculate M9 supplemented with D-glucose, L-arabinose, L- ribose, or D-gluconate, a
198 longer lag phase was observed, but a similar biomass to wild type was reached **(Fig.**
199 **2A-C)**.
200 Next, we constructed a Δ*cyaB*/Δ*cyaA* double mutant strain by deleting *cyaA* from
201 the Δ*cyaB* background. The double mutant demonstrated small translucent colony
202 morphology on LBS similar to the colonies observed for Δ*crp* **(Fig. S2A)**. Interestingly, a
203 plate streaked on LBS from the glycerol stock gave small translucent colonies and
204 regular opaque colonies, suggesting suppressor mutations were occurring. We did not
205 see this phenotype in either of the single *cya* mutants (**Fig. S2B**). Addition of cAMP to
206 the media restored the large colony morphology for the double mutant (**Fig. S2B-D**). In
207 *V. cholerae,* which contains only the AC-I CyaA, the Δ*cyaA* mutant reversion to wild-
208 type phenotypes was also observed (12). For our analysis, small colonies were always
209 used for characterization studies. The Δ*cyaB*/Δ*cyaA* double mutant showed a growth

210 defect on M9S D-glucose (**Fig. 1B**) and showed no growth in M9 supplemented with L-
211 arabinose, L-ribose, or D-gluconate **(Fig. 2A-C)**. The growth assays were performed in
212 M9S L-arabinose, L-ribose, or D-gluconate with inoculum obtained after overnight
213 growth in M9S D-glucose. These growth assays showed that the Δ*cyaA* mutant grew
214 similar to wild type, but the Δ*cyaB* mutant had a significantly longer lag phase.
215 However, when strains were grown overnight in LBS and then inoculated into
216 alternative carbon sources, the Δ*cyaB* mutant showed a shorter lag phase and a
217 significantly greater biomass than the Δ*cyaA* mutant, which grew similar to wild type
218 (**Fig. 4**). This suggest that *cyaA* is under CRP control and that *cyaB* is not under
219 catabolite repression. Analysis of the regulatory regions of both genes identified
220 putative CRP binding sites in the regulatory region of *cyaA* but not *cyaB* (data not
221 shown). The growth assays also demonstrate that CyaB functions as an adenylate
222 cyclase and CyaA and CyaB can complement each other.
223 **CRP regulation of swimming and swarming motility**.
224 *Vibrio parahaemolyticus* produces both polar and lateral flagella required for swimming
225 and swarming motility, respectively (43). To investigate the role of CRP in *V.*
226 *parahaemolyticus* motility, we conducted swimming assays and found that the Δ*crp*
227 mutant was defective in swimming compared to wild type but did not show a complete
228 defect similar to the Δ*rpoN* mutant (**Fig. 5A**). Similarly, the Δ*crp* mutant also showed a
229 defect in swarming as indicated by the absence of the budding phenotype compared to

230 wild type (**Fig. 5B**). Neither of the single Δ*cyaA* nor Δ*cyaB* mutants showed a motility
231 defect, however the Δ*cyaB*/Δ*cyaA* double mutant showed defects similar to Δ*crp* (**Fig. 5A**
232 **and 5B**). These data demonstrate that the cAMP-CRP is required for motility of *V.*
233 *parahaemolyticus*.

234 **CRP and CyaB required for CPS and biofilm production.**

235 Capsule polysaccharide (CPS) production is a key component of biofilm and is
236 positively controlled by the quorum sensing master regulator OpaR in *V.*
237 *parahaemolyticus* (34, 36, 38-40, 44). To determine whether CRP plays a role in CPS
238 formation, we examined the Δ*crp* and *cya* mutants on HI medium supplemented with
239 congo red and $CaCl_2$, incubated for 48 hrs at 30˚C. The wild type strain produced a
240 rugose opaque colony as did the Δ*cyaA* mutant, indicative of CPS production (**Fig. 6**).
241 However, the Δ*cyaB* mutant produced a smooth translucent colony indicative of the
242 absence of CPS. The Δ*crp and* Δ*cyaB*/Δ*cyaA* mutants also did not produce CPS,
243 presenting a smooth translucent colony morphology (**Fig. 6**). These data show that CRP
244 is a positive regulator of CPS production and *cyaB* is also essential. In biofilm assays, a
245 similar pattern emerged as seen with CPS, where the Δ*cyaA* mutant produce a biofilm
246 similar to wild type, however both the Δ*crp* and Δ*cyaB* mutants produced significantly
247 less biofilm (**Fig. 7**). Overall, these data demonstrate that both CRP and CyaB, but not
248 CyaA, are required for CPS and biofilm production in *V. parahaemolyticus*.

249 **Distribution and phylogenetic analysis of *cyaB*.**

250 CyaB was first identified in a strain of *A. hydrophila, Y. pestis,* and a number of
251 hyperthermophilic archaebacterial (21). We used *cyaB* (VP1760) as a seed and examined
252 the distribution among members of the family *Vibrionaceae* in the NCBI genome
253 database. The *cyaB* gene was present in all *V. parahaemolyticus* strains and was highly
254 conserved. CyaB was absent from most *V. alginolyticus* strains, a closely related species
255 to *V. parahaemolyticus*, but was present in other members of the Harveyi clade to which
256 *V. parahaemolyticus* belongs, such as *V. campbellii, V. harveyi, V. jasicida, V. owensii, and V.*
257 *rotiferanus* (**Fig. 8**). These species showed ~70% amino acid identity with CyaB, but ~95%
258 amino acid identity to CyaA from *V. parahaemolyticus*. On the *cyaB* gene tree, within the
259 Harveyi clade, species formed two divergent branches, one branch representing *V.*
260 *parahaemolyticus* strains and the second branching pattern representing the other
261 species. This suggests that *cyaB* in *V. parahaemolyticus* has diverged significantly from
262 *cyaB* in the other Harveyi clade species. Of note is a *cyaB* gene from a strain of *V.*
263 *alginolyticus*, which is present on a plasmid that clusters within the same group as *cyaB*
264 from *V. coralliilyticus*, which is also present on a plasmid (**Fig. 8**). This suggest that in
265 these strains and species, *cyaB* was acquired by horizontal gene transfer. In general, the
266 *cyaB* gene from the genera *Aliivibrio* and *Photobacterium* cluster closely together and are
267 divergent from *Vibrio* species, as one would expect if the gene is ancestral to the groups
268 (**Fig. 8**). However, *cyaB* from five *Photobacterium* species clustered within *Vibrio* clades
269 indicating that these *Photobacterium* species acquired a copy of the *cyaB* gene from

270 *Vibrio*, another example of horizontal gene transfer of *cyaB* in these groups (**Fig. 8**).
271 Comparison of CyaA phylogeny with the CyaB phylogeny from the same set of species
272 also demonstrated additional instances of horizontal transfer of *cyaB* among species
273 shown by the non-congruency of the branching patterns for several CyaB proteins (**Fig.**
274 **S4**).

275 **DISCUSSION**

276 Here we describe the physiological role of a class IV adenylate cyclase (AC). In this
277 study, we demonstrated that in *V. parahaemolyticus*, CRP is an important regulator of
278 metabolism and motility, acting as a positive regulator of both swimming and
279 swarming motility. In addition, we showed that CRP is a positive regulator of CPS and
280 biofilm formation. Multiple studies in *E. coli* and enterobacteria, in general, have
281 demonstrated that deleting *cyaA* impairs the cell's cAMP production thus deactivating
282 CRP, which led to Δ*cyaA* and Δ*crp* mutants demonstrating identical phenotypes (45, 46).
283 In *V. cholerae* and *V. vulnificus,* deletion of *cyaA* gave phenotypes identical to Δ*crp,*
284 showing defects in metabolism and motility (17, 47, 48). In our study in *V.*
285 *parahaemolyticus,* the Δ*cyaA* mutant showed phenotypes similar to wild type. This
286 unexpected finding prompted us to search for proteins with putative AC function in the
287 *V. parahaemolyticus* genome and led us to identify *cyaB* (VP1760). CyaB belongs to CYTH
288 superfamily of proteins, a class IV AC, which contains one domain. The canonical AC
289 CyaA, which is a class I type, contains two domains: a cyclase domain and a regulatory
290 domain. CyaB contains a single domain and a homolog was previously identified in *A.*

291 *hydrophila*, *Y. pestis* and hyperthermophilic archaebacteria (21, 22, 41, 42). In *A.*
292 *hydrophila*, CyaB was only active at high temperatures and alkaline pH conditions and
293 not active under normal laboratory condition (21). In that study, it was demonstrated
294 that deleting *cyaB* did not show any cAMP-CRP phenotypic defects. However, when
295 *cyaB* was expressed from a plasmid in the Δ*cyaA* and Δ*cyaA*/Δ*cyaB* mutant strains, it was
296 able to restore the phenotypes back to wild type (21). No physiological role for CyaB
297 has been uncovered. In contrast, in our study, deleting *cyaB* showed defects in
298 metabolism, CPS production, and biofilm formation similar to the Δ*crp* mutant, but with
299 less severity. This indicates that CyaB is important for these phenotypes and that CyaA
300 could be compensating for the loss of CyaB. The double mutant Δ*cyaB*/Δ*cyaA*
301 demonstrated phenotypes identical to Δ*crp* indicating that only after removing both
302 CyaA and CyaB, the cells became devoid of cAMP.
303 Under optimal growth conditions in M9S D-glucose, deleting *cyaA* did not have
304 any impact on CRP function, thus we do not see any phenotypic changes. However,
305 deleting *cyaB* showed growth differences absent in the Δ*cyaA* mutant. When the Δ*cyaB*
306 mutant was grown overnight in M9S D-glucose, cell growth was impaired on non-PTS
307 sugars, presenting as a longer lag phase, suggesting in these cells *cyaA* was repressed
308 and needs time to adjust to non-PTS sugars. However, when the Δ*cyaB* mutant is grown
309 overnight in LBS, cells are primed for growth on non-PTS sugars, as *cyaA* is expressed
310 in LBS and these cells show significantly better growth and shorter lag phases than
311 either wild type or the Δ*cyaA* mutant. To investigate this further, bioinformatics analysis

312 was used to identify the putative CRP binding sites in the regulatory region of *cyaA* and
313 *cyaB.* We identified putative CRP binding sites in the regulatory region of *cyaA*, one of
314 which overlaps the RNAP binding site, characteristic of a repressor (data not shown).
315 No CRP binding sites were identified in the regulatory region of *cyaB*, suggesting that
316 this gene is regulated differently than *cyaA*. The data also suggest that the presence of
317 *cyaB* may have a negative impact on growth since the Δ*cyaB* mutant grows better than
318 wild type and the Δ*cyaA* mutant. The differences between the Δ*cyaA* and Δ*cyaB* mutants
319 will likely be explained in terms of differences in expression and activation of these
320 enzymes in response to specific environmental signals.

321 The defects in CPS production and biofilm formation in both the Δ*crp* and Δ*cyaB*
322 mutants indicate that cAMP-CRP is a positive regulator of these phenotypes and CyaB
323 is essential for this function. Studies in *V. cholerae* identified cAMP-CRP as a negative
324 regulator of capsule production and biofilm formation (17, 49). These studies showed
325 that cAMP-CRP negatively regulated vibrio polysaccharide (VPS) genes and biofilm
326 matrix proteins. The quorum sensing regulator HapR was also shown to negatively
327 regulate these phenotypes in *V. cholerae* (50-52). In *V. cholerae*, *vsp* gene regulation is
328 negatively controlled by HapR and it was shown that *crp* was epistatic to *hapR* in the
329 regulation of *vspT* and *vspR* regulators of VSP production (17, 49-52). It is of interest to
330 note that both a Δ*crp* and Δ*cyaA* mutants showed decreased expression of *hapR*
331 indicating that CRP is a positive regulator of HapR (16, 17, 49). In *V. parahaemolyticus*,

332 the quorum sensing regulator OpaR is a positive regulator of CPS and biofilm,
333 however, whether cAMP-CRP controls OpaR is unknown. Our preliminary
334 bioinformatics analysis idenitifed putative CRP binding sites in the regulator region of
335 OpaR suggesting CRP is may also regulated opaR in *V. parahaemolyticus*, which will
336 need to be investigated further.

337 **MATERIALS AND METHODS**

338 **Bacterial strains, media, and culture conditions.**

339 All strains and plasmids used in this study are listed in **Table 1**. A streptomycin-
340 resistant clinical isolate *V. parahaemolyticus* RIMD2210633 was used throughout the
341 study. Unless stated otherwise, all *V. parahaemolyticus* strains were grown in Luria
342 Bertani (LB) medium (Fischer Scientific, Pittsburgh, PA) containing 3% NaCl (LBS) at
343 37°C with aeration or M9 medium media (Sigma Aldrich, St. Louis, MO) containing 3%
344 NaCl (M9S) supplement with 10mM of various carbon sources. Antibiotics were added
345 to growth media at the following concentrations: Ampicillin (Amp), 100 μg/ml,
346 streptomycin (Sm), 200 μg/ml, chloramphenicol (Cm), 10 μg/ml, and kanamycin (Km),
347 50 μg/ml when required.

348 **Construction of mutant strains in *V. parahaemolyticus* RIMD2210633.**

349 Splice by overlapping extension (SOE) PCR and an allelic exchange (53) was used to
350 construct in-frame, non-polar deletion mutants of *crp* (VP2793), *cyaA* (VP2987), *cyaB*
351 (VP1760) and double deletion *cyaB*/*cyaA* in *V. parahaemolyticus* RIMD2210633. Primer

352 pairs were designed for *crp* (VP2793), *cyaA* (VP2987), and *cyaB* (VP1760) PCR
353 amplification using *V. parahaemolyticus* RIMD2210633 genomic DNA as a template. All
354 primers used in this study are listed in **Table S1**. Using the PCR amplified fragments of
355 each gene, SOE PCR was conducted to obtain truncated version of *crp* (81-bps of 633-bp
356 VP2793), *cyaA* (153-bp of 2,529-bp VP2987) and *cyaB* (84-bp of 546-bp VP1760). The
357 truncated PCR fragments were cloned into the suicide vector pDS132 and named
358 pDS*Δcrp*, pDS*ΔcyaA*, and pDS*ΔcyaB*. pDS*Δcrp*, pDS*ΔcyaA*, and pDS*ΔcyaB* were
359 transformed into *E. coli* strain β2155 *λpir*, which were conjugated separately into *V.*
360 *parahaemolyticus*. Conjugation was conducted by spread plating both strains onto LBS
361 plate containing 0.3 mM diaminopimelic acid (DAP). Bacterial growth from this plate
362 was scrapped, suspended in LBS, serially diluted, and plated on LBS plates containing
363 streptomycin and chloramphenicol. After overnight growth, colonies were examined to
364 identify single crossovers of the suicide plasmids into the target site via PCR. The
365 colonies with single crossover were grown over night in LBS with no antibiotic and
366 plated onto LBS plate containing 10% sucrose to select for double crossover deletion
367 mutant. The double deletion mutant Δ*cyaB*/Δ*cyaA* was constructed by deleting *cyaA*
368 from Δ*cyaB* background following the above protocol. The gene deletions were
369 confirmed by PCR and DNA sequencing.
370 **Functional complementation of *E. coli* Δ*cyaA*.**

371 Primer pairs were designed to amplify *cyaA* (VP2987) and *cyaB* (VP1760) using wild
372 type genomic DNA as template (**Table S1**). Purified PCR products of *cyaA* and *cyaB*,
373 and the vector pBBR1MCS were digested using BamHI and XbaI. Both the insert and
374 the vector were gel purified. The genes were each cloned into the vector pBBR1MCS
375 creating pBB*cyaA* or pBB*cyaB*, which were then transformed into *E. coli* B2155 using the
376 calcium chloride transformation method. *E. coli* β2155 containing pBB*cyaA* and pBB*cyaB*
377 were transformed into *E. coli* Δ*cyaA* (54). The transformed complementation strain was
378 selected for using LB agar supplemented with Km and Cm. Complement strains were
379 verified using PCR and sequencing. IPTG (0.5mM) was used to induce the transcription
380 of the respective genes from the vector.

381 **Growth pattern analysis.**

382 Bacterial cultures were grown overnight in LBS or M9S supplemented with 10mM
383 glucose at 37°C with aeration. An overnight growth culture was spun down,
384 resuspended, and washed with PBS and a 1: 40 dilution was then used to conduct
385 growth pattern analysis in M9S supplemented with 10 mM of each individual carbon
386 sources. Growth curves were performed in a 96 well plate at 37°C with aeration. Optical
387 density (OD595) was measured each hour for 24 hours. The data was plotted using
388 GraphPad Prism 7.00, GraphPad software, La Jolla, California USA,
389 www.graphpad.com.

390 **Swimming and Swarming motility assay.**

391 Swimming assays were performed in semi-solid media, LB 2% NaCl with 0.3% agar and
392 swarming assays were performed in heart infusion (HI) medium (Remel, Lenexa, KS)
393 containing 2% NaCl and 1.5 % agar. To examine swimming behavior, a single colony of
394 the test bacterium was picked and stabbed in the center of the LB plate and incubated at
395 37°C for 24 hrs. For the swarming assay, a single colony was picked and gently
396 inoculated on the surface of the HI plate, and the plates were incubated at 30°C for 48
397 hrs.

398 **Capsule polysaccharide production assay.**

399 Capsule polysaccharide (CPS) formation assays were conducted as previously
400 described (55, 56). Wild type and mutants of interest were grown on HI media
401 containing 1.5% agar, 2% NaCl, 2.5 mM $CaCl_2$, and 0.25% Congo red dye for 48 hrs at
402 30°C. Each image is an example from at least three biological replicates.

403 **Biofilm formation assay.**

404 Biofilm assays were performed as previously described (39, 40, 57). Briefly, overnight
405 cultures were used to inoculate strip wells in a 1:40 dilution in LBS. Cultures were
406 incubated for 24 hrs at 37°C prior to analysis. Biofilm was stained with crystal violet and
407 solubilized with dimethyl sulfoxide (DMSO) (ThermoFisher Scientific, USA). Optical
408 density was measured at 595nm to quantify biofilm.

409 **Phylogenetic analysis of *cyaB*.**

410 pBLAST searches with VP1760 from *V. parahaemolyticus* used as a seed were performed
411 on all completed and draft *Vibrionaceae* genomes published on the National Center for
412 Biotechnology Institute (NCBI) website. Sequences were aligned using CLUSTALW
413 (58). Phylogenetic analysis was conducted with MEGA X(59). The evolutionary history
414 was inferred by using the Maximum Likelihood method and Kimura 2-parameter
415 model (60). The tree with the highest log likelihood (-16932.68) is shown. The
416 percentage of trees in which the associated taxa clustered together is shown next to the
417 branches. Initial tree(s) for the heuristic search were obtained automatically by applying
418 Neighbor-Join and BioNJ algorithms to a matrix of pairwise distances estimated using
419 the Maximum Composite Likelihood (MCL) approach, and then selecting the topology
420 with superior log likelihood value. A discrete Gamma distribution was used to model
421 evolutionary rate differences among sites (3 categories (+*G*, parameter = 0.5711)). The
422 tree is drawn to scale, with branch lengths measured in the number of substitutions per
423 site. This analysis involved 61 nucleotide sequences. Codon positions included were
424 1st+2nd+3rd. All positions with less than 95% site coverage were eliminated, that is
425 fewer than 5% alignment gaps, missing data, and ambiguous bases were allowed at any
426 position (partial deletion option). There were a total of 543 positions in the final dataset.
427 For the species that contained CyaB, a second tree was constructed for the same set of
428 species based on CyaA protein sequences and compared with the CyaA tree for
429 differences in branching patterns amongst species.

**ACKNOWLEDGMENTS**

This research was supported in part by a National Science Foundation grant (award IOS-1656688) to E.F.B. J.G.T was funded by a University of Delaware graduate fellowship award.

434 **REFERENCES:**


435 1. Botsford JL, Harman JG. 1992. Cyclic AMP in prokaryotes. Microbiol Rev 56:100-
436 22.

437 2. Stülke J, Hillen W. 1999. Carbon catabolite repression in bacteria. Curr Opin
438 Microbiol 2:195-201.

439 3. Kolb A, Busby S, Buc H, Garges S, Adhya S. 1993. Transcriptional regulation by
440 cAMP and its receptor protein. Annu Rev Biochem 62:749-95.

441 4. Zheng D, Constantinidou C, Hobman JL, Minchin SD. 2004. Identification of the
442 CRP regulon using in vitro and in vivo transcriptional profiling. Nucleic Acids
443 Res 32:5874-93.

444 5. Benoff B, Yang H, Lawson CL, Parkinson G, Liu J, Blatter E, Ebright YW, Berman
445 HM, Ebright RH. 2002. Structural basis of transcription activation: the CAP-alpha
446 CTD-DNA complex. Science 297:1562-6.

447 6. Lawson CL, Swigon D, Murakami KS, Darst SA, Berman HM, Ebright RH. 2004.
448 Catabolite activator protein: DNA binding and transcription activation. Curr
449 Opin Struct Biol 14:10-20.

450 7. Berg OG, von Hippel PH. 1988. Selection of DNA binding sites by regulatory
451 proteins. II. The binding specificity of cyclic AMP receptor protein to recognition
452 sites. J Mol Biol 200:709-23.

453 8. Shimada T, Fujita N, Yamamoto K, Ishihama A. 2011. Novel roles of cAMP
454 receptor protein (CRP) in regulation of transport and metabolism of carbon
455 sources. PLoS One 6:e20081.
456 9. Popovych N, Tzeng SR, Tonelli M, Ebright RH, Kalodimos CG. 2009. Structural
457 basis for cAMP-mediated allosteric control of the catabolite activator protein.
458 Proc Natl Acad Sci U S A 106:6927-32.
459 10. Bârzu O, Danchin A. 1994. Adenylyl cyclases: a heterogeneous class of ATP-
460 utilizing enzymes. Prog Nucleic Acid Res Mol Biol 49:241-83.
461 11. Ramakrishnan G, Jain A, Chandra N, Srinivasan N. 2016. Computational
462 recognition and analysis of hitherto uncharacterized nucleotide cyclase-like
463 proteins in bacteria. Biol Direct 11:27.
464 12. Skorupski K, Taylor RK. 1997. Control of the ToxR virulence regulon in *Vibrio*
465 *cholerae* by environmental stimuli. Mol Microbiol 25:1003-1009. .
466 13. Kovacikova G, Skorupski K. 2001. Overlapping binding sites for the virulence
467 gene regulators AphA, AphB and cAMP-CRP at the Vibrio cholerae tcpPH
468 promoter. Mol Microbiol 41:393-407.
469 14. Li CC, Crawford JA, DiRita VJ, Kaper JB. 2000. Molecular cloning and
470 transcriptional regulation of ompT, a ToxR-repressed gene in Vibrio cholerae.
471 Mol Microbiol 35:189-203.

472 15. Li CC, Merrell DS, Camilli A, Kaper JB. 2002. ToxR interferes with CRP-
473 dependent transcriptional activation of ompT in Vibrio cholerae. Mol Microbiol
474 43:1577-89.
475 16. Silva AJ, Pham K, Benitez JA. 2003. Haemagglutinin/protease expression and
476 mucin gel penetration in El Tor biotype Vibrio cholerae. Microbiology 149:1883-
477 1891.
478 17. Liang W, Pascual-Montano A, Silva AJ, Benitez JA. 2007. The cyclic AMP
479 receptor protein modulates quorum sensing, motility and multiple genes that
480 affect intestinal colonization in Vibrio cholerae. Microbiology (Reading) 153:2964-
481 2975.
482 18. Ladant D, Ullmann A. 1999. Bordatella pertussis adenylate cyclase: a toxin with
483 multiple talents. Trends Microbiol 7:172-6.
484 19. Sinha SC, Sprang SR. 2006. Structures, mechanism, regulation and evolution of
485 class III nucleotidyl cyclases. Rev Physiol Biochem Pharmacol 157:105-40.
486 20. Smith RS, Wolfgang MC, Lory S. 2004. An adenylate cyclase-controlled signaling
487 network regulates Pseudomonas aeruginosa virulence in a mouse model of acute
488 pneumonia. Infect Immun 72:1677-84.
489 21. Sismeiro O, Trotot P, Biville F, Vivares C, Danchin A. 1998. Aeromonas
490 hydrophila adenylyl cyclase 2: a new class of adenylyl cyclases with thermophilic

491 properties and sequence similarities to proteins from hyperthermophilic
492 archaebacteria. J Bacteriol 180:3339-44.
493 22. Smith N, Kim SK, Reddy PT, Gallagher DT. 2006. Crystallization of the class IV
494 adenylyl cyclase from Yersinia pestis. Acta Crystallogr Sect F Struct Biol Cryst
495 Commun 62:200-4.
496 23. Charania MA, Brockman KL, Zhang Y, Banerjee A, Pinchuk GE, Fredrickson JK,
497 Beliaev AS, Saffarini DA. 2009. Involvement of a membrane-bound class III
498 adenylate cyclase in regulation of anaerobic respiration in Shewanella oneidensis
499 MR-1. J Bacteriol 191:4298-306.
500 24. Cotta MA, Whitehead TR, Wheeler MB. 1998. Identification of a novel adenylate
501 cyclase in the ruminal anaerobe, Prevotella ruminicola D31d. FEMS Microbiol
502 Lett 164:257-60.
503 25. Téllez-Sosa J, Soberón N, Vega-Segura A, Torres-Márquez ME, Cevallos MA.
504 2002. The Rhizobium etli cyaC product: characterization of a novel adenylate
505 cyclase class. J Bacteriol 184:3560-8.
506 26. Skorupski K, Taylor RK. 1997. Cyclic AMP and its receptor protein negatively
507 regulate the coordinate expression of cholera toxin and toxin-coregulated pilus in
508 Vibrio cholerae. Proc Natl Acad Sci U S A 94:265-70.
509 27. Matson JS, Withey JH, DiRita VJ. 2007. Regulatory networks controlling Vibrio
510 cholerae virulence gene expression. Infect Immun 75:5542-9.

511 28. Beyhan S, Bilecen K, Salama SR, Casper-Lindley C, Yildiz FH. 2007. Regulation of
512 rugosity and biofilm formation in Vibrio cholerae: comparison of VpsT and VpsR
513 regulons and epistasis analysis of vpsT, vpsR, and hapR. J Bacteriol 189:388-402.
514 29. Manneh-Roussel J, Haycocks JRJ, Magán A, Perez-Soto N, Voelz K, Camilli A,
515 Krachler AM, Grainger DC. 2018. cAMP Receptor Protein Controls Vibrio
516 cholerae Gene Expression in Response to Host Colonization. mBio 9.
517 30. Colwell RR, Kaper JB, Joseph A. 1977. Vibrio cholerae, Vibrio parahaemolyticus,
518 and other vibrios: occurrence and distribution in Chesapeake. Science 198:394-
519 396.
520 31. Joseph SW, Colwell RR, Kaper JB. 1982. *Vibrio parahaemolyticus* and related
521 halophilic *Vibrios.* Crit Rev Microbiol 10:77-124.
522 32. DePaola A, Kaysner CA, Bowers J, Cook DW. 2000. Environmental investigations
523 of Vibrio parahaemolyticus in oysters after outbreaks in Washington, Texas, and
524 New York (1997 and 1998). Appl Environ Microbiol 66:4649-54.
525 33. Nair G, Ramamurthy T, Bhattacharya S, Dutta B, Takeda Y, Sack D. 2007. Global
526 dissemination of *Vibrio parahaemolyticus* serotype O3:K6 and its serovariants. Clin
527 Microbiol Rev 20:39-48
528 34. McCarter LL. 1998. OpaR, a homolog of Vibrio harveyi LuxR, controls opacity of
529 Vibrio parahaemolyticus. J Bacteriol 180:3166-73.

530 35. Enos-Berlage JL, McCarter LL. 2000. Relation of capsular polysaccharide
531 production and colonial cell organization to colony morphology in Vibrio
532 parahaemolyticus. J Bacteriol 182:5513-20.
533 36. Kernell Burke A, Guthrie LT, Modise T, Cormier G, Jensen RV, McCarter LL,
534 Stevens AM. 2015. OpaR controls a network of downstream transcription factors
535 in Vibrio parahaemolyticus BB22OP. PLoS One 10:e0121863.
536 37. Gode-Potratz CJ, McCarter LL. 2011. Quorum sensing and silencing in Vibrio
537 parahaemolyticus. J Bacteriol 193:4224-37.
538 38. Guvener ZT, McCarter LL. 2003. Multiple regulators control capsular
539 polysaccharide production in Vibrio parahaemolyticus. J Bacteriol 185:5431-41.
540 39. Kalburge SS, Carpenter MR, Rozovsky S, Boyd EF. 2017. Quorum Sensing
541 Regulators Are Required for Metabolic Fitness in Vibrio parahaemolyticus. Infect
542 Immun 85.
543 40. Tague JG, Hong J, Kalburge SS, Boyd EF. 2022. Regulatory Small RNA Qrr2 Is
544 Expressed Independently of Sigma Factor-54 and Can Function as the Sole Qrr
545 Small RNA To Control Quorum Sensing in Vibrio parahaemolyticus. J Bacteriol
546 204:e0035021.
547 41. Gallagher DT, Kim SK, Robinson H, Reddy PT. 2011. Active-site structure of
548 class IV adenylyl cyclase and transphyletic mechanism. J Mol Biol 405:787-803.

549 42. Gallagher DT, Smith NN, Kim SK, Heroux A, Robinson H, Reddy PT. 2006.
550 Structure of the class IV adenylyl cyclase reveals a novel fold. J Mol Biol 362:114-
551 22.
552 43. Whitaker WB, Richards GP, Boyd EF. 2014. Loss of sigma factor RpoN increases
553 intestinal colonization of *Vibrio parahaemolyticus* in an adult mouse model. Infect
554 Immun 82:544-56.
555 44. Enos-Berlage JL, Guvener ZT, Keenan CE, McCarter LL. 2005. Genetic
556 determinants of biofilm development of opaque and translucent Vibrio
557 parahaemolyticus. Mol Microbiol 55:1160-82.
558 45. Hufnagel DA, Evans ML, Greene SE, Pinkner JS, Hultgren SJ, Chapman MR.
559 2016. The Catabolite Repressor Protein-Cyclic AMP Complex Regulates csgD and
560 Biofilm Formation in Uropathogenic Escherichia coli. J Bacteriol 198:3329-3334.
561 46. Kalivoda EJ, Stella NA, O'Dee DM, Nau GJ, Shanks RM. 2008. The cyclic AMP-
562 dependent catabolite repression system of Serratia marcescens mediates biofilm
563 formation through regulation of type 1 fimbriae. Appl Environ Microbiol
564 74:3461-70.
565 47. Kim YR, Kim SY, Kim CM, Lee SE, Rhee JH. 2005. Essential role of an adenylate
566 cyclase in regulating Vibrio vulnificus virulence. FEMS Microbiol Lett 243:497-
567 503.

568 48. Kim YR, Lee SE, Kim B, Choy H, Rhee JH. 2013. A dual regulatory role of cyclic
569 adenosine monophosphate receptor protein in various virulence traits of Vibrio
570 vulnificus. Microbiol Immunol 57:273-80.
571 49. Fong JCN, Yildiz FH. 2008. Interplay between Cyclic AMP-Cyclic AMP Receptor
572 Protein and Cyclic di-GMP Signaling in Vibrio cholerae Biofilm Formation.
573 Journal of Bacteriology 190:6646-6659.
574 50. Hammer BK, Bassler BL. 2003. Quorum sensing controls biofilm formation in
575 Vibrio cholerae. Mol Microbiol 50:101-4.
576 51. Zhu J, Mekalanos JJ. 2003. Quorum sensing-dependent biofilms enhance
577 colonization in Vibrio cholerae. Dev Cell 5:647-56.
578 52. Yildiz FH, Liu XS, Heydorn A, Schoolnik GK. 2004. Molecular analysis of
579 rugosity in a Vibrio cholerae O1 El Tor phase variant. Mol Microbiol 53:497-515.
580 53. Ho SN, Hunt HD, Horton RM, Pullen JK, Pease LR. 1989. Site-directed
581 mutagenesis by overlap extension using the polymerase chain reaction. Gene
582 77:51-9.
583 54. Baba T, Ara T, Hasegawa M, Takai Y, Okumura Y, Baba M, Datsenko KA, Tomita
584 M, Wanner BL, Mori H. 2006. Construction of Escherichia coli K-12 in-frame,
585 single-gene knockout mutants: the Keio collection. Mol Syst Biol 2:2006.0008.
586 55. Güvener Z, McCarter L. 2003. Multiple regulators control capsular
587 polysaccharide production in *Vibrio parahaemolyticus*. J Bacteriol 185:5431-41.

588 56. Kalburge SS, Carpenter MR, Rozovsky S, Boyd EF. 2017. Quorum sensing
589 regulators are required for metabolic fitness in *Vibrio parahaemolyticus*. Infect
590 Immun 85:930-16.
591 57. Tague JG, Regmi A, Gregory GJ, Boyd EF. 2021. Fis Connects Two Sensory
592 Pathways, Quorum Sensing and Surface Sensing, to Control Motility in Vibrio
593 parahaemolyticus. Front Microbiol 12:669447.
594 58. Thompson JD, Higgins DG, Gibson TJ. 1994. CLUSTAL W: improving the
595 sensitivity of progressive multiple sequence alignment through sequence
596 weighting, position-specific gap penalties and weight matrix choice. Nucleic
597 Acids Res 22:4673-80.
598 59. Kumar S, Stecher G, Li M, Knyaz C, Tamura K. 2018. MEGA X: Molecular
599 Evolutionary Genetics Analysis across Computing Platforms. Mol Biol Evol
600 35:1547-1549.
601 60. Kimura M. 1980. A simple method for estimating evolutionary rates of base
602 substitutions through comparative studies of nucleotide sequences. J Mol Evol
603 16:111-20.
604 61. Makino K, Oshima K, Kurokawa K, Yokoyama K, Uda T, Tagomori K, Iijima Y,
605 Najima M, Nakano M, Yamashita A, Kubota Y, Kimura S, Yasunaga T, Honda T,
606 Shinagawa H, Hattori M, Iida T. 2003. Genome sequence of *Vibrio*

607 *parahaemolyticus*: a pathogenic mechanism distinct from that of *V. cholerae*. Lancet
608 361:743-9.
609 62. Grenier F, Matteau D, Baby V, Rodrigue S. 2014. Complete Genome Sequence of
610 Escherichia coli BW25113, Genome Announc, vol 2.
611
612
613
614

615 **Table 1. Bacterial strains and plasmids used in this study**

| **Bacterial strains** | **Genotype or description** | **References or sources** |
|---|---|---|
| ***Vibrio parahaemolyticus*** | | |
| RIMD2210633 | O3:K6 clinical isolate, $Sm^r$ | (61) |
| Δ*crp* | RIMD2210633 Δ*crp* (VP2793), $Sm^r$ | This study |
| Δ*cyaA* | RIMD2210633 Δ*cyaA* (VP2987), $Sm^r$ | This study |
| Δ*cyaB* | RIMD2210633 Δ*cyaB* (VP1760), $Sm^r$ | This study |
| Δ*cyaB*/Δ*cyaA* | RIMD2210633 Δ*cyaB* Δ*cyaA* (VP2987), $Sm^r$ | This study |
| Δ*rpoN* | RIMD2210633 Δ*rpoN* (VP2670), $Sm^r$ | (43) |
| ***Escherichia coli*** | | |
| BW25113 | Wild-Type *E. coli* K12 strain | (62) |
| Δ*cyaA* | BW25113, F-, *Δ(araD-araB)567, ΔlacZ4787(::rrnB-3), λ⁻, rph-1, ΔcyaA751::kan, Δ(rhaD-rhaB)568, hsdR514* | |
| DH5αλpir | | Laboratory collection |
| B2155λpir | *ΔdapA::emr pir*, for bacterial conjugation | Laboratory collection |
| B2155pDS*crp* | B2155 strain harboring pDS*crp* | This study |
| B2155pDS*cyaA* | B2155 strain harboring pDS*cyaA* | This study |
| B2155pDS*cyaB* | B2155 strain harboring pDS*cyaB* | This study |
| **Complement strains** | | This study |
| *E. coli* Δ*cyaA*pCyaA | *E. coli* Δ*cyaA* harboring pBBR*cyaA* | This study |
| *E. coli* Δ*cyaA*pCyaB | *E. coli* Δ*cyaA* harboring pBBRcyaA | This study |
| **Plasmids** | | |
| pDS132 | Suicide plasmid, $Cm^r$, SacB | |
| pDSΔ*crp* | pDS132 harboring truncated *crp*, $Cm^r$ | This study |
| pDSΔ*cyaA* | pDS132 harboring truncated *cyaA*, $Cm^r$ | This study |
| pDSΔ*cyaB* | pDS132 harboring truncated *cyaB*, $Cm^r$ | This study |
| pBBR1MCS | Expression vector, lacZ promoter, $Cm^r$ | This study |
| pBBR*cyaA* | pBBR1MCS harboring full-length *cyaA* (VP2987), $Cm^r$ | This study |
| pBBR*cyaB* | pBBR1MCS harboring full-length *cyaB*(VP1760), $Cm^r$ | This study |

616

617

618 **Figure Legends**

619 **Fig. 1. Growth pattern analysis in LBS and M9S D-Glucose.** Growth pattern analysis
620 of *V. parahaemolyticus* RIMD2210633 (closed circle), Δ*cyaA* (open circle), Δ*cyaB* (open
621 square), Δ*cyaB*/Δ*cyaA* (open triangle) and Δ*crp* (closed downward facing triangle) in **(A)**
622 LBS **(B)** M9S + 10mM D-glucose at 37°C with aeration for 24 hrs. For growth in minimal
623 media (M9), the strains were grown overnight in M9 3%NaCl (M9S) + 10mM glucose
624 (M9GS) at 37°C with aeration for 24 hrs.

625 **Fig. 2. Growth pattern analysis in alternative carbon sources.** Growth pattern analysis
626 of *V. parahaemolyticus* (closed circle), Δ*cyaA* (open circle), Δ*cyaB* (open square),
627 Δ*cyaB*/Δ*cyaA* (open triangle) and Δ*crp* (closed downward facing triangle) in **(A)** M9S +
628 10mM L-arabinose, **(B)** M9S + L-ribose **(C)** M9S + 10mM D-gluconate at 37°C with
629 aeration for 24 hrs. Inoculums were grown overnight in M9S + 10mM glucose at 37°C
630 with aeration.

631 **Fig. 3: Complementation analysis of *E. coli* Δ*cyaA*.** The *E. coli* Δ*cyaA* strain was
632 complemented separately with a functional copy of *cyaA* and *cyaB* from *V.*
633 *parahaemolyticus* and growth curves were conducted in **(A)** M9 + 10 mM glucose **(B)** M9
634 + 10mM gluconate for 48 hrs at 37°C with aeration.

635 **Fig. 4. Growth pattern analysis in alternative carbon sources.** Growth pattern analysis
636 of *V. parahaemolyticus* (closed circle), Δ*cyaA* (open circle), Δ*cyaB* (open square),
637 Δ*cyaB*/Δ*cyaA* (open triangle) and Δ*crp* (closed downward facing triangle) in **(A)** M9S +

638 10mM L-arabinose, **(B)** M9S + L-ribose **(C)** M9S + 10mM D-gluconate at 37°C with

639 aeration for 24 hrs. Inoculums were grown overnight in LBS at 37°C with aeration.

640 **Fig. 5. Characterization of motility in *V. parahaemolyticus* mutants. (A)** Swimming

641 assays were conducted using wild type, Δ*crp*, Δ*cyaA*, Δ*cyaB*, and Δ*cyaB*/Δ*cyaA* mutants

642 grown at 37°C for 24 hrs. The diameter of the region covered by the bacterial strains

643 were measured and represented as bar graph **(B**) Swarming assays. Colonies of wild

644 type and mutant strains Δ*crp*, Δ*cyaA*, Δ*cyaB*, and Δ*cyaB*/Δ*cyaA* were assessed for

645 swarming motility in semi solid media over 48 hrs.

646 **Fig. 6. Capsule polysaccharide production**. Colonies of *V. parahaemolyticus*

647 RIMD2210633 and mutant strains were inoculated on HI plate containing Congo red

648 dye and grown at 37°C for 24 hrs.

649 **Fig. 7. Biofilm formation**. *V. parahaemolyticus* strains were grown for 24 hrs in HI broth.

650 The biofilms were visualized using crystal violet and then dissolved using DMSO, and

651 the optical density of the biofilms were measured at OD (600) and represented as bar

652 graphs. Error bars indicate standard error of mean (SEM). Unpaired Student *t* test was

653 conducted to obtain the *P* values. The significant difference in biofilm production is

654 denoted by asterisks. *, $P<0.05$, **, $P<0.01$, ***, $P<0.001$. NS, not significant.

655 **Fig. 8. Evolutionary analysis by Maximum Likelihood method of *cyaB***. Evolutionary

656 analyses were conducted in MEGA X. The evolutionary history was inferred by using

657 the Maximum Likelihood method and Kimura 2-parameter model. A discrete Gamma

658 distribution was used to model evolutionary rate differences among sites (5 categories
659 (+*G*, parameter = 0.5599)). The tree is drawn to scale, with branch lengths measured in
660 the number of substitutions per site. A discrete Gamma distribution was used to model
661 evolutionary rate differences among sites (3 categories (+*G*, parameter = 0.5711)). The
662 tree is drawn to scale, with branch lengths measured in the number of substitutions per
663 site. This analysis involved 61 nucleotide sequences. Codon positions included were
664 1st+2nd+3rd. All positions with less than 95% site coverage were eliminated (partial
665 deletion option). There was a total of 543 positions in the final dataset.
666
667

668 **Supplementary Data**

669 **Table S1.**

| Primer name and use | Sequence (5′-3′)[a] | Melting temp (°C) | Size (bp) |
|---|---|---|---|
| **SOE PCR** | | | |
| VP1760 SOEA | GGATCTAGACAGCTCAACTGGGTTTGGTT | 62 | 408 |
| VP1760 SOEB | TTCAAACTGCCCTTGGAAATG | 54 | |
| VP1760 SOEC | CATTTCCAAGGGCAGTTTGAAGAAGCGGA TAGAGAGCATCG | 66 | 513 |
| VP1760 SOED | CACGAGCTCGCTGCTTATCTTTGCGCTTT | 64 | |
| VP1760 SOEFF | ACGGTGAAAGCCATCAAAAC | 54 | 1,708 |
| VP1760 SOEFR | CCTTCGGTCTTACAATAACCAATC | 54 | |
| VP2793 SOEA | TCTAGATTGTGGTGATTCGTCTGCGT | 60 | 458 |
| VP2793 SOEB | TGTTGGGTCGGTTTGAGGTT | 57 | |
| VP2793 SOEC | AACCTCAAACCGACCCAACACTAATCTCT GCGCACGGTAA | 68 | 451 |
| VP2793 SOED | GCATGCCCATCTTCGTCAAGCAGGGT | 65 | |
| VP2793 SOEFF | CTGCACACCTTTGACGAAGC | 57 | 2,408 |
| VP2793 SOEFR | GAGTCGTTATGACGCCCGAT | 57 | |
| VP2987 SOEA | TCTAGACAGGATGAGCGGCTTGAAGA | 61 | 513 |
| VP2987 SOEB | GCGATCGATACGCTGCTGGTT | 60 | |
| VP2987 SOEC | **AACCAGCAGCGTATCGATCGC**CACCCTG AAGAGGGTAACGC | 71 | 503 |
| VP2987 SOED | GAGCTCGCACCACACTCAGGAAAAGC | 64 | |
| VP2987 SOEFF | CGCACCTTGAGGGAGTTCAT | 57 | 4,042 |
| VP2987 SOEFR | GAGGATGTTGACCCACAGCA | 57 | |
| **Complementation** | | | |
| *cyaA* com F | CAAGGATCCTGTTCAACCAAGGAATTACC C | 61 | 2,563 |
| *cyaA* com R | GCATCTAGAGGATATGTTTACGTTACGCG | 59 | |
| *cyaB* com F | CTTGGATCCAGTTTATGTAGTAGAGGCGA | 59 | 576 |
| *cyaB* com R | CACTCTAGAGAAATAGCGACTATGCTGAT | 57 | |

[a]Underlined base pairs indicate restriction sites

670

671

672 **Fig. S1. Genomic context comparison of *crp*, *cyaA* and *cyaB* loci.** The genomic region
673 upstream and downstream of **(A)** *crp* and **(B)** *cyaA* **(C)** *cyaB* from *V. parahaemolyticus* was
674 compared with that of *crp* and *cyaA* from *V. cholerae*, *V. vulnificus* and *E. coli* and *cyaB*
675 from *V. harveyi* using tBLASTx, and figures were constructed using Easyfig.
676 **Fig. S2. Colony Morphology of *Vibrio parahaemolyticus* strains. A.** Single colony of *V.*
677 *parahaemolyticus* RIMD2210633 and its isogenic mutant strains Δ*cyaA*, Δ*cyaB*,
678 Δ*cyaB*/Δ*cyaA,* and Δ*crp* were plated on LBS agar plate and grown overnight at 37$^{o}$C
679 before the picture was taken. **B.** An inoculum from the glycerol stock of Δ*cyaB*/Δ*cyaA*
680 was plated on LBS agar and grown overnight at 37 $^{o}$C showing small and large
681 colonies. **C.** Comparison of Wild type (WT) and double mutant *cyaB/cyaA*. **D**. Addition
682 of 1mM cAMP restores large colony morphology to *cyaB/cyaA*.
683 **Fig. S3: CyaB amino acid sequence and crystal structure. A.** Alignment of CyaB among
684 *Aeromonas hydrophila, V. parahaemolyticus and Yersinia pestis.*
685 **Fig. S4**. **Phylogenetic comparison of CyaA and CyaB trees**. The CyaA tree ws
686 constructed using proteins sequences from the same set of species that contained CyaB.
687 Lines between the two trees of similar color represent species that cluster together on
688 the CyaA tree.
689
690

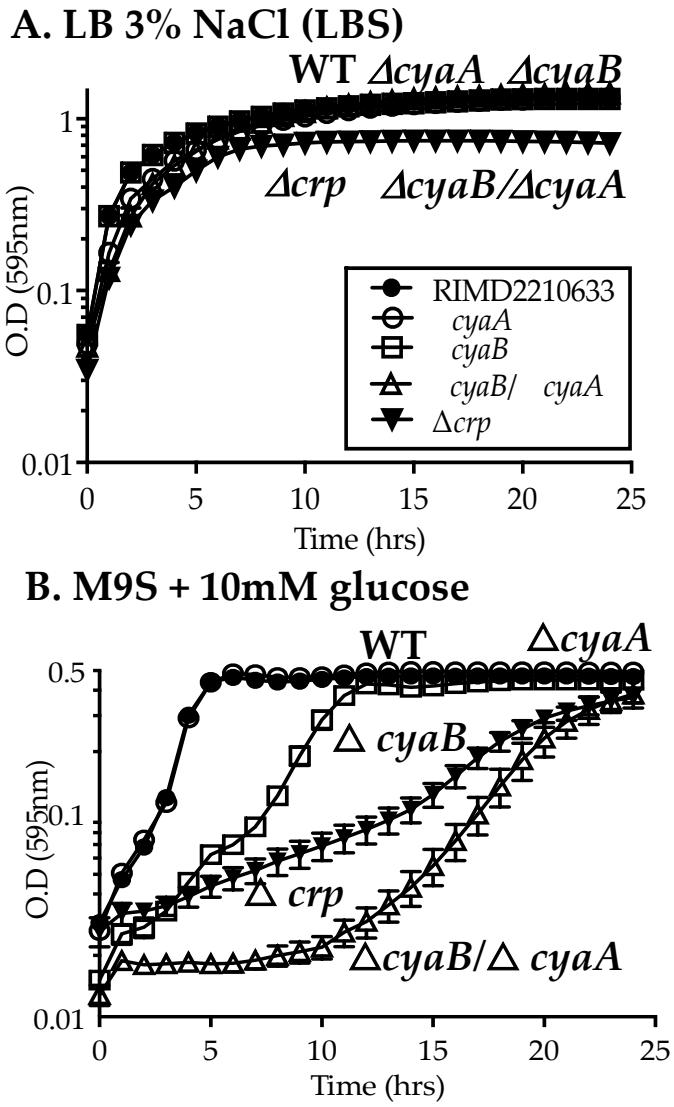
A. LB 3% NaCl (LBS)
WT ΔcyaA ΔcyaB
Δcrp ΔcyaB/ΔcyaA
RIMD2210633
cyaA
cyaB
cyaB/ cyaA
Δcrp
O.D (595nm)
1
0.1
0.01
0
5
10
15
20
25
Time (hrs)
B. M9S + 10mM glucose
WT
ΔcyaA
Δ cyaB
Δ crp
ΔcyaB/Δ cyaA
O.D (595nm)
0.5
0.1
0.01
0
5
10
15
20
25
Time (hrs)

**Fig. 1**

**A. M9S + 10mM L-arabinose**

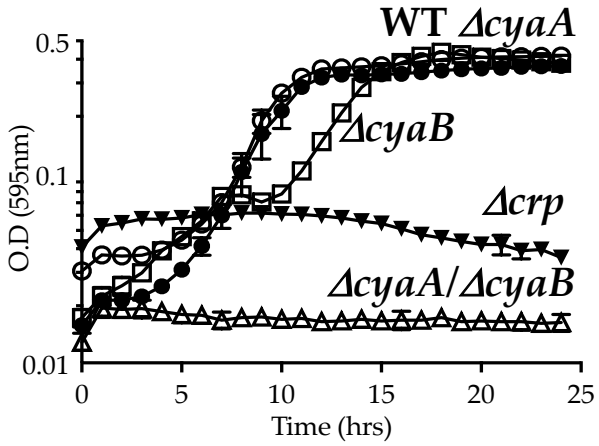


**B. M9S + 10mM L-ribose**

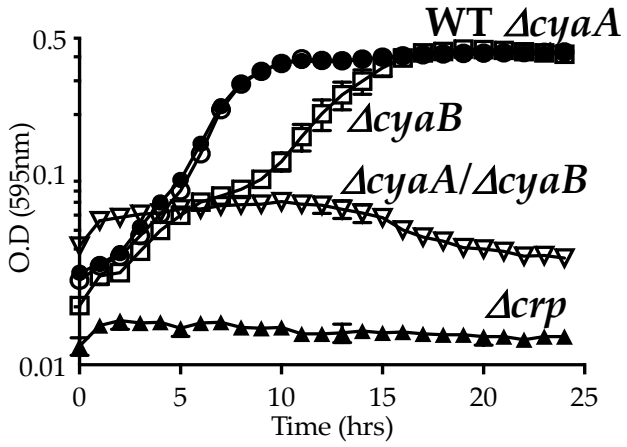


**C. M9S + 10mM D-gluconate**

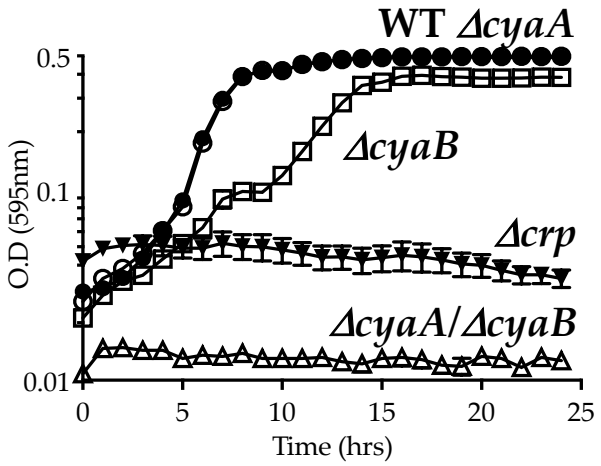


**Fig. 2**

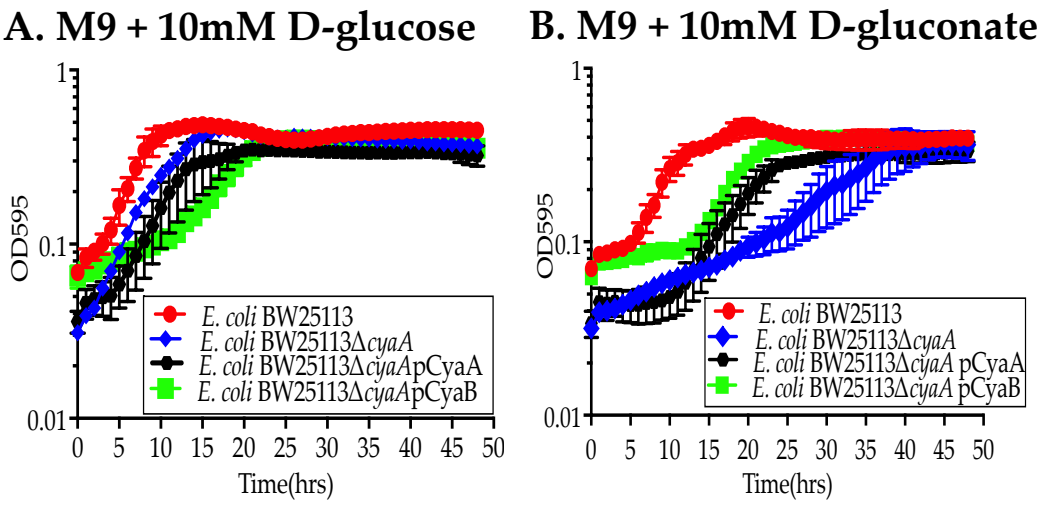
A. M9 + 10mM D-glucose
B. M9 + 10mM D-gluconate
OD595
1
0.1
0.01
0 5 10 15 20 25 30 35 40 45 50
Time(hrs)
E. coli BW25113
E. coli BW25113ΔcyaA
E. coli BW25113ΔcyaApCyaA
E. coli BW25113ΔcyaApCyaB
E. coli BW25113ΔcyaA pCyaA
E. coli BW25113ΔcyaA pCyaB

**Fig. 3**

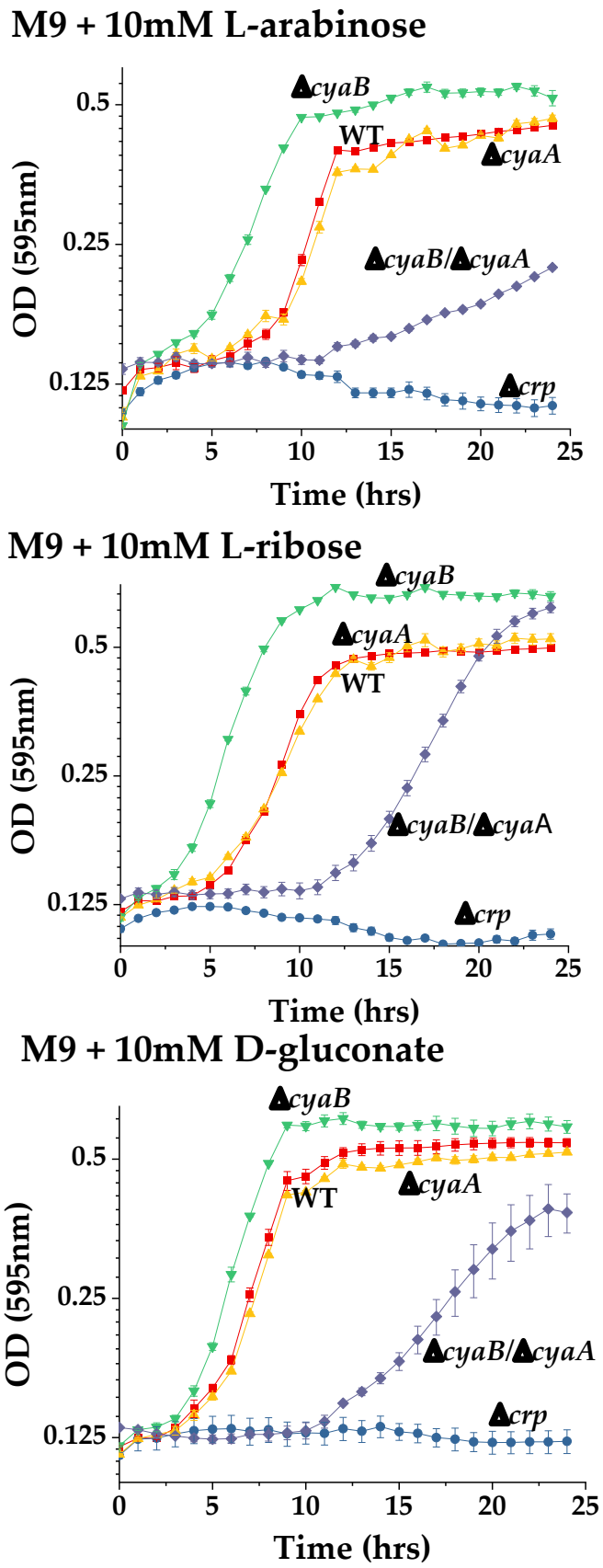
M9 + 10mM L-arabinose
ΔcyaB
WT
ΔcyaA
ΔcyaB/ΔcyaA
Δcrp
OD (595nm)
0.5
0.25
0.125
0
5
10
15
20
25
Time (hrs)
M9 + 10mM L-ribose
ΔcyaB
ΔcyaA
WT
ΔcyaB/ΔcyaA
Δcrp
OD (595nm)
0.5
0.25
0.125
0
5
10
15
20
25
Time (hrs)
M9 + 10mM D-gluconate
ΔcyaB
WT
ΔcyaA
ΔcyaB/ΔcyaA
Δcrp
OD (595nm)
0.5
0.25
0.125
0
5
10
15
20
25
Time (hrs)

**Fig. 4**

**A. Swimming motility**

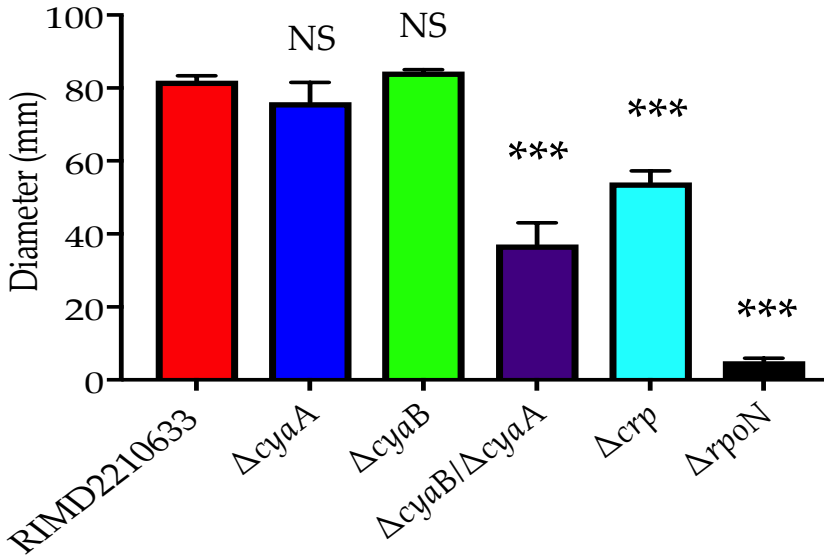


**B. Swarming motility**

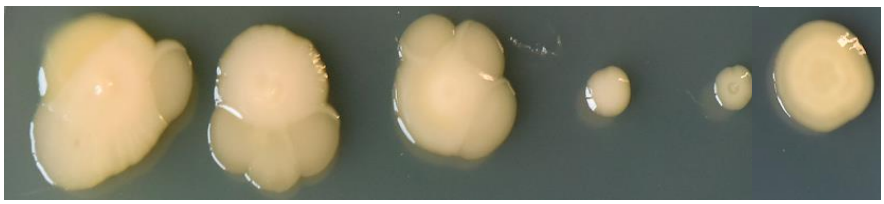

**WT** **Δ*cyaA*** **Δ*cyaB*** **Δ*cyaB*/ Δ*cyaA*** **Δ*crp*** **Δ*rpoN***

**Fig. 5**

**Capsule polysaccharide (CPS) production**

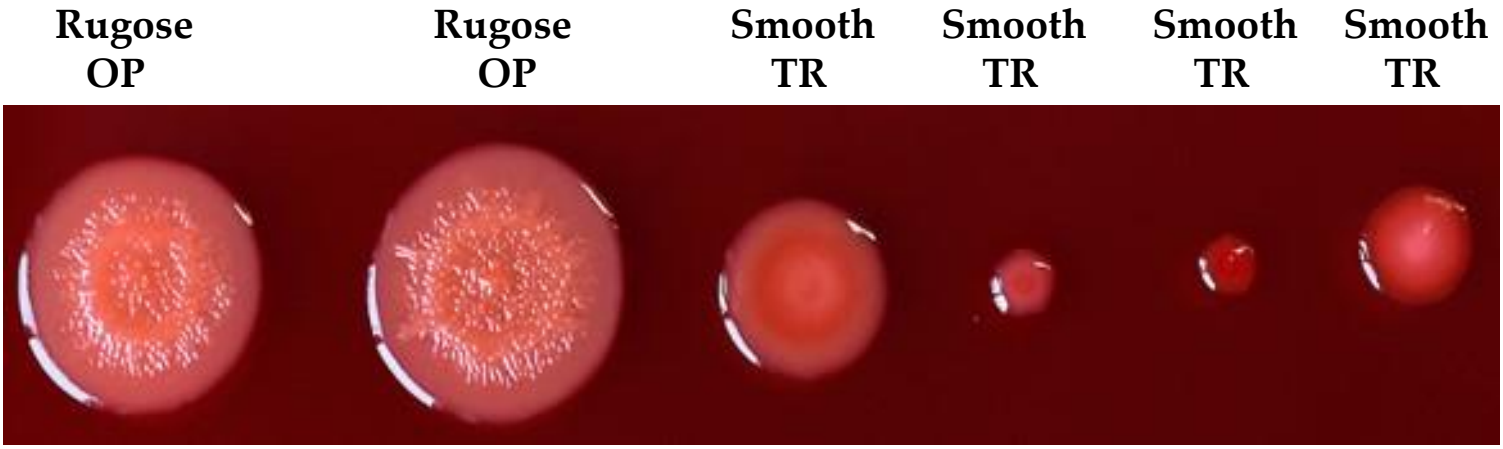


**Fig. 6**

**A. Biofilm formation assay**

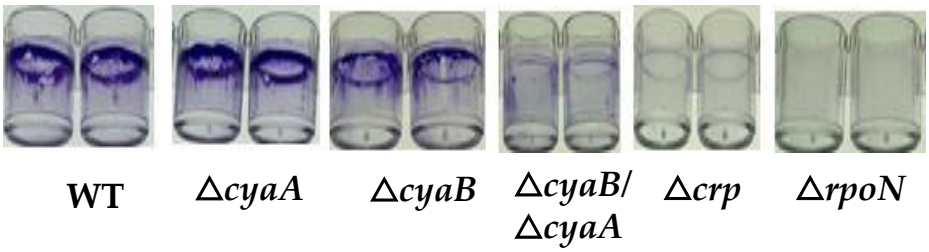


**B. Biofilm quantification**

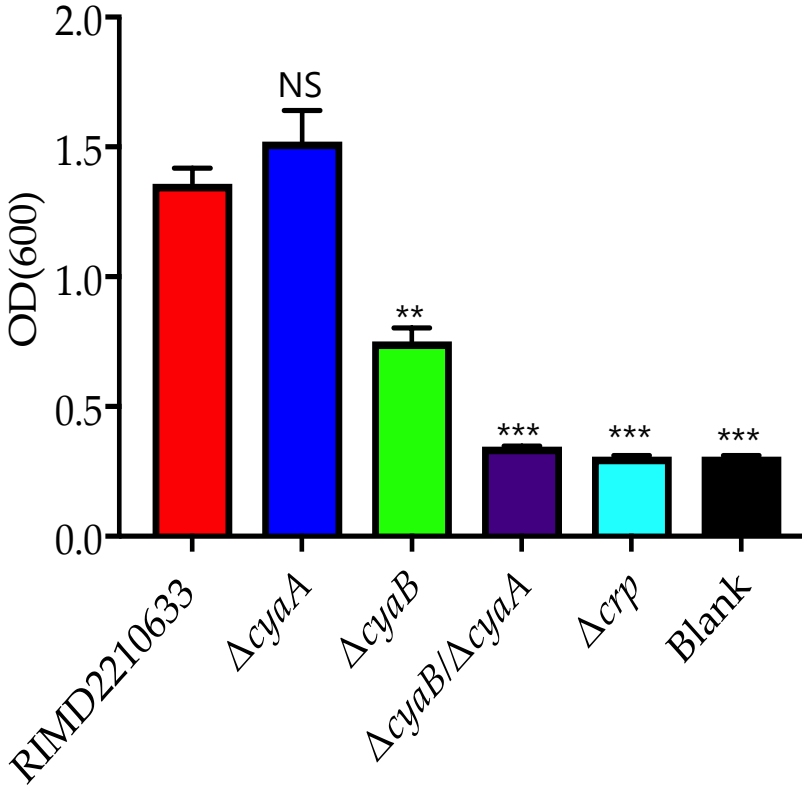


**Fig. 7**

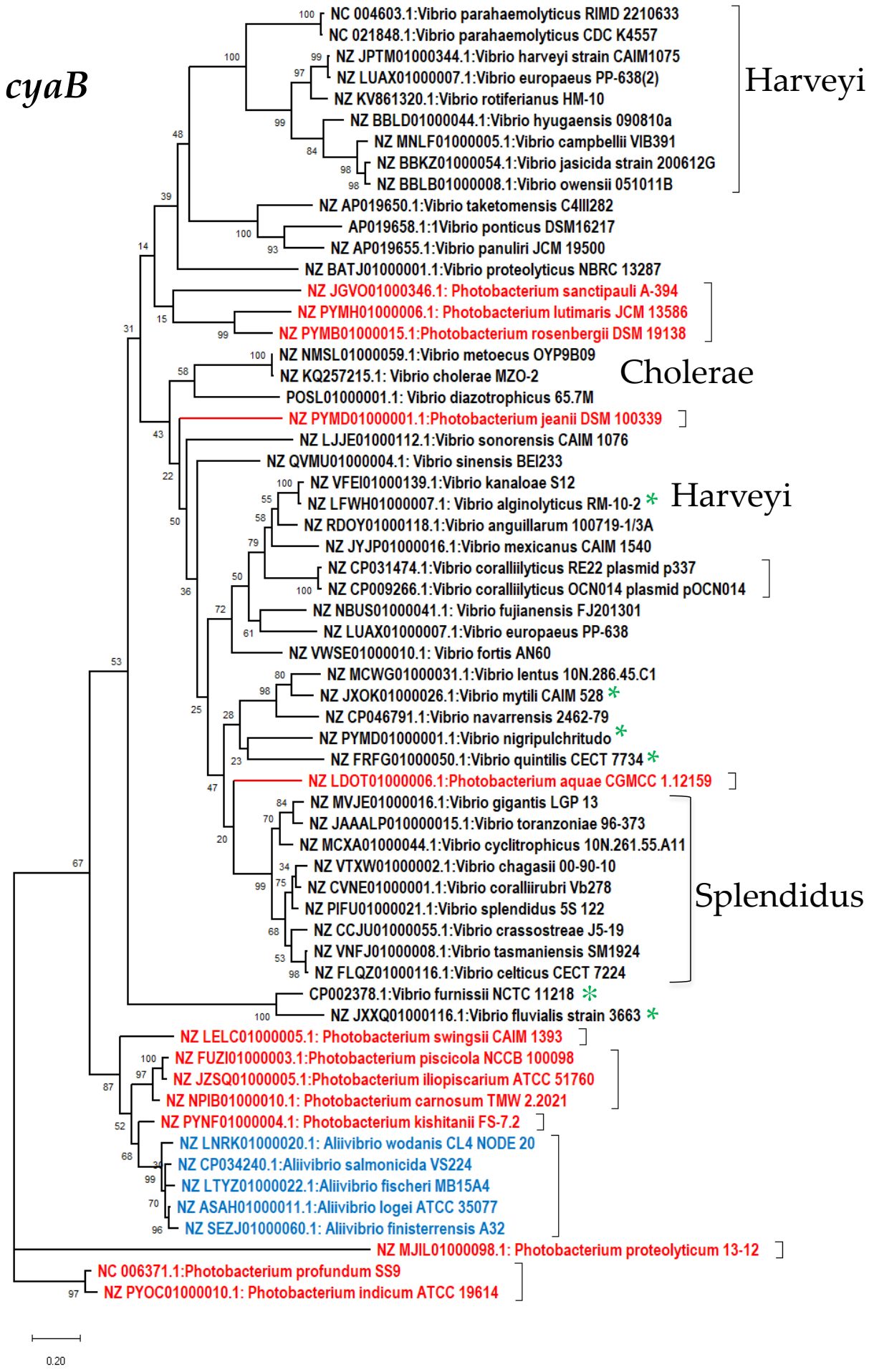
cyaB
NC 004603.1:Vibrio parahaemolyticus RIMD 2210633
NC 021848.1:Vibrio parahaemolyticus CDC K4557
NZ JPTM01000344.1:Vibrio harveyi strain CAIM1075
NZ LUAX01000007.1:Vibrio europaeus PP-638(2)
NZ KV861320.1:Vibrio rotiferianus HM-10
NZ BBLD01000044.1:Vibrio hyugaensis 090810a
NZ MNLF01000005.1:Vibrio campbellii VIB391
NZ BBKZ01000054.1:Vibrio jasicida strain 200612G
NZ BBLB01000008.1:Vibrio owensii 051011B
Harveyi
NZ AP019650.1:Vibrio taketomensis C4III282
AP019658.1:1Vibrio ponticus DSM16217
NZ AP019655.1:Vibrio panuliri JCM 19500
NZ BATJ01000001.1:Vibrio proteolyticus NBRC 13287
NZ JGVO01000346.1: Photobacterium sanctipauli A-394
NZ PYMH01000006.1: Photobacterium lutimaris JCM 13586
NZ PYMB01000015.1:Photobacterium rosenbergii DSM 19138
NZ NMSL01000059.1:Vibrio metoecus OYP9B09
NZ KQ257215.1: Vibrio cholerae MZO-2
Cholerae
POSL01000001.1: Vibrio diazotrophicus 65.7M
NZ PYMD01000001.1:Photobacterium jeanii DSM 100339
NZ LJJE01000112.1:Vibrio sonorensis CAIM 1076
NZ QVMU01000004.1: Vibrio sinensis BEI233
NZ VFEI01000139.1:Vibrio kanaloae S12
NZ LFWH01000007.1: Vibrio alginolyticus RM-10-2 *
Harveyi
NZ RDOY01000118.1:Vibrio anguillarum 100719-1/3A
NZ JYJP01000016.1:Vibrio mexicanus CAIM 1540
NZ CP031474.1:Vibrio coralliilyticus RE22 plasmid p337
NZ CP009266.1:Vibrio coralliilyticus OCN014 plasmid pOCN014
NZ NBUS01000041.1: Vibrio fujianensis FJ201301
NZ LUAX01000007.1:Vibrio europaeus PP-638
NZ VWSE01000010.1: Vibrio fortis AN60
NZ MCWG01000031.1:Vibrio lentus 10N.286.45.C1
NZ JXOK01000026.1:Vibrio mytili CAIM 528 *
NZ CP046791.1:Vibrio navarrensis 2462-79
NZ PYMD01000001.1:Vibrio nigripulchritudo *
NZ FRFG01000050.1:Vibrio quintilis CECT 7734 *
NZ LDOT01000006.1:Photobacterium aquae CGMCC 1.12159
NZ MVJE01000016.1:Vibrio gigantis LGP 13
NZ JAAALP010000015.1:Vibrio toranzoniae 96-373
NZ MCXA01000044.1:Vibrio cyclitrophicus 10N.261.55.A11
NZ VTXW01000002.1:Vibrio chagasii 00-90-10
NZ CVNE01000001.1:Vibrio coralliirubri Vb278
NZ PIFU01000021.1:Vibrio splendidus 5S 122
NZ CCJU01000055.1:Vibrio crassostreae J5-19
NZ VNFJ01000008.1:Vibrio tasmaniensis SM1924
NZ FLQZ01000116.1:Vibrio celticus CECT 7224
Splendidus
CP002378.1:Vibrio furnissii NCTC 11218 *
NZ JXXQ01000116.1:Vibrio fluvialis strain 3663 *
NZ LELC01000005.1: Photobacterium swingsii CAIM 1393
NZ FUZI01000003.1:Photobacterium piscicola NCCB 100098
NZ JZSQ01000005.1:Photobacterium iliopiscarium ATCC 51760
NZ NPIB01000010.1: Photobacterium carnosum TMW 2.2021
NZ PYNF01000004.1: Photobacterium kishitanii FS-7.2
NZ LNRK01000020.1: Aliivibrio wodanis CL4 NODE 20
NZ CP034240.1:Aliivibrio salmonicida VS224
NZ LTYZ01000022.1:Aliivibrio fischeri MB15A4
NZ ASAH01000011.1:Aliivibrio logei ATCC 35077
NZ SEZJ01000060.1: Aliivibrio finisterrensis A32
NZ MJIL01000098.1: Photobacterium proteolyticum 13-12
NC 006371.1:Photobacterium profundum SS9
NZ PYOC01000010.1: Photobacterium indicum ATCC 19614
0.20

**Fig. 8**